



HAL
open science

Effect of the injection of water-containing diluents on band broadening in analytical supercritical fluid chromatography

Magali Batteau, Karine Faure

► **To cite this version:**

Magali Batteau, Karine Faure. Effect of the injection of water-containing diluents on band broadening in analytical supercritical fluid chromatography. *Journal of Chromatography A*, 2022, 1673, pp.463056. 10.1016/j.chroma.2022.463056 . hal-03711565

HAL Id: hal-03711565

<https://hal.science/hal-03711565>

Submitted on 20 Oct 2022

HAL is a multi-disciplinary open access archive for the deposit and dissemination of scientific research documents, whether they are published or not. The documents may come from teaching and research institutions in France or abroad, or from public or private research centers.

L'archive ouverte pluridisciplinaire **HAL**, est destinée au dépôt et à la diffusion de documents scientifiques de niveau recherche, publiés ou non, émanant des établissements d'enseignement et de recherche français ou étrangers, des laboratoires publics ou privés.

1 Effect of the injection of water-containing diluents on band broadening in analytical 2 supercritical fluid chromatography

3
4 Magali Batteau¹, Karine Faure¹

5 ¹Université de Lyon, CNRS, Université Claude Bernard Lyon 1, Institut des Sciences Analytiques,
6 UMR 5280, 5 rue de la Doua, F-69100 VILLEURBANNE, France

7 *Corresponding author: karine.faure@isa-lyon.fr
8
9

10 Abstract

11 In this study, the impact of introducing water in the sample solvent upon the injection in SFC is
12 investigated. Adsorption of water on the stationary phase was indicated. Using a set of ten neutral test
13 compounds and four ionizable test compounds, spread all along the co-solvent gradient, several
14 parameters were scrutinized (i.e. water content in the sample diluent, nature of the sample diluent,
15 nature of the co-solvent) in regards to peak broadening. From this systematic investigation, the
16 competition for adsorption on the stationary phase between the analytes and the water molecules
17 contained in the diluent was highlighted. The chromatographic peaks of neutral molecules eluting
18 before water molecules were compressed and the ones eluting after were broadened. While the extent
19 of this phenomenon was related to the peak position for neutral molecules, it was not observed on
20 acidic molecules.

21 Keywords

22 Supercritical fluid chromatography; sample diluent; injection; peak broadening
23
24

25 1. Introduction

26 In analytical SFC, the injection is performed after the co-solvent and the CO₂ are mixed at initial
27 proportions. Hence the injection plug is located in a zone usually rich in CO₂ and a viscosity mismatch
28 is frequent. Moreover, the nature of the sample diluent is of major importance on the peak shape. The
29 selection of the sample diluent is hence of great concern. For polar SFC stationary phases, aprotic
30 and low viscosity solvents, such as MtBE, are recommended to avoid the formation of viscous
31 fingering as well as any strong solvent effects [1].

32 However, for the past few years, the application area of SFC is growing interest towards more polar
33 solutes which may experience solubility issues in aprotic solvents. The use of polar co-solvents in SFC
34 eases the analysis of polar metabolites, sugars or peptides [2], for which water is usually the best
35 solubilizing diluent. Another interesting development for SFC is its implementation as a second
36 dimension in a two-dimensional chromatographic separation. This combination opens new
37 opportunities, thanks to the large orthogonality it provides [3, 4], while it may impose the transfer of
38 hydro-organic fractions into the SFC dimension.

39 The presence of water and eventually MeOH is known to be highly detrimental to SFC peak shapes,
40 as these solvents both present elevated viscosity and polarity, contrasting with the initial CO₂-rich
41 mobile phase. So far, solutions consisted in injecting very low sample volumes. But Enmark et al.

42 highlighted that deformations can even happen at very low injection volume, starting at 0.3 % column
43 volume [5]. Using specific flow-through needle injectors that increment the sample plug with a feed
44 solvent has shown recently to be able to reduce the impact of MeOH diluent on the separation [6], but
45 water as a diluent was not investigated. On the other hand, the situation where SFC is online with an
46 LC instrument is even more demanding. In an online LC x SFC configuration, loops of large volume
47 need to be used to allow sufficient time for the ²D separation to be conducted. Moreover, the loops
48 need to be fully filled to avoid residual air gaps, that may result from the decompression of the ²D
49 mobile phase in the loop, to be injected [7]. This leads to the injection of a large amount of ¹D mobile
50 phase into the ²D SFC dimension. Previous online hyphenation of LC with SFC avoided the water
51 injection issue by removing the LC eluent through packed loop interfaces [8-10], or by injecting very
52 low volumes into the SFC column [7]. While the first solution is highly effective, the risk of carry-over
53 exists. On the other hand, the transfer of low volume is quite demanding in online two-dimensional
54 separations, imposing a drastic reduction of the ¹D flow-rate. A better understanding of water impact
55 upon injection in SFC is hence required.

56 Lastly, one can notice that studies focusing on injection effects of water-containing diluents in SFC
57 have been performed under isocratic mode so far [5, 7, 11]. However, gradient elution is known to
58 favor robustness in SFC [12] and is increasingly applied to separate analytes covering a wider range
59 of polarity [13].

60 The goal of this experimental study was to conduct a systematic investigation of the influence of
61 several parameters on band broadening when injecting samples dissolved in a water-containing
62 diluent. These parameters included the position of the analyte peak, the water content in the injection
63 solvent as well as the nature of the organic solvent injected along. The nature of the co-solvent and
64 the presence of additives in this co-solvent were also investigated.

65

66 **2. Materials and methods**

67 **2.1 Chemicals, reagents and columns**

68 All standards had a purity exceeding 95%. The following standards were obtained from Sigma Aldrich
69 (Germany): eugenol, 2,4,6-trimethylphenol, 1-indanol, apocynin, o-cresol, m-cresol, phenol, 4-
70 hydroxybenzyl alcohol, naringenin, acrylic acid, imipramine hydrochloride and propranolol
71 hydrochloride. Arbutin, trans-cinnamic acid and ferulic acid were obtained from Fluka (UK), Sigma
72 Acros Organic (USA) and Sarsyntex (France), respectively.

73 Methanol (MeOH) ($\geq 99.8\%$), ethanol ($> 98\%$) and formic acid ($> 98\%$) were purchased from Fisher
74 Scientific (UK), acetonitrile (ACN) ($\geq 99.9\%$) was purchased from Honeywell (Germany), methyl tert-
75 butyl ether (MtBE) ($\geq 99.9\%$) was purchased from Acros Organics (USA).

76 Ultrapure water was delivered by PURELAB Classic system from Elga (UK) (18.2 M Ω -cm).
77 Ammonium hydroxide solution was ACS reagent (28.0-30.0 % NH₃ basis) purchased from Sigma-
78 Aldrich (Germany). Pressurized carbon dioxide (CO₂) (N45, $\geq 99,995\%$) was purchased from Air
79 Liquide (France).

80 Three columns were assessed, Torus DEA and Torus Diol with dimensions 100 x 3.0 mm, 1.7 μ m and
81 BEH HILIC with dimensions 100 x 2.1 mm; 1.7 μ m, all from Waters (Milford, USA).

82 **2.2 SFC instrument**

83 All experiments were performed on an Agilent 1260 Infinity II SFC (Agilent, USA) equipped with a
84 SFC-binary pump (G4782A), an oven column 1260 MCT (G7116A), a detector 1260 DAD WR
85 (G7115A) equipped with a SFC flow cell (400 bars, 2 μL , 3 mm path length) and a 1260 SFC control
86 module (G4301A). To mimic the full loop injection that may occur during online LC x SFC, the
87 commercial flow-through needle (FTN) injector was reverted to a fixed-loop model. The instrument
88 was modified to accommodate a SFC-Autosampler (G4303A) with a fixed injection loop of either 5 μL ,
89 10 μL or 20 μL volume. The instrumental variance due to extra column was estimated at 37 μL^2 (liquid
90 conditions) and at 12 μL^2 (for 5 % co-solvent). The dwell volume, excluding loop volume, was 780 μL .

91 **2.3 Sample preparation**

92 A stock solution of each standard was prepared at 20 mg/mL or 20 $\mu\text{L}/\text{mL}$ in MeOH. Using the stock
93 solutions, a mixture containing several compounds at a final concentration between 0.05 to 0.2 mg/mL
94 (according to their UV response) in either MtBE, or ACN/water with various ratio, or MeOH /water with
95 various ratio, except for imipramine prepared at 1 mg/mL.

96 **2.4 Chromatographic conditions**

97 Samples were injected with an injection volume of 5 μL , 10 μL or 20 μL (full loop with overfill factor
98 x2). The flow rate was 1.4 mL/min, so that the instrumental pressure remains below 400 bars during
99 gradient. The initial composition of the mobile phase was 95 % CO_2 / 5 % organic co-solvent (v/v), with
100 a linear gradient up to a final composition of 50 % co-solvent, with a gradient time of 5.3 min
101 (normalized gradient slope of 2 %). Then the column returned to the initial composition in 0.3 min
102 (corresponding to one void volume) and was reconditioned with initial conditions for 2 min. Back-
103 pressure was maintained constant at 140 bar. The column oven temperature was set at 40 $^{\circ}\text{C} \pm 0.8$
104 $^{\circ}\text{C}$. UV detection was set at 220 nm (bandwidth 4 nm, frequency 40 Hz) unless stated otherwise. The
105 instrument was controlled by OpenLab CDS ChemStation C01.08 (Agilent). Ammonium hydroxide (20
106 mM) was added to the co-solvent to avoid peak tailing when analysing basic compounds [14].
107

108 **2.5 Selection of test compounds and column.**

109 While most studies on injection effect focus on poorly retained analytes, it seemed important to select
110 compounds across the whole elution range while limiting the number of variables. A set of 10 neutral
111 test compounds, with log P ranging from -0.6 to 2.2 was investigated, selected among lignin-derived
112 compounds. Two smaller sets containing three acidic compounds and two basic compounds
113 completed the study (Table 1).

114
115 Diethylamine column (DEA) was selected as providing the largest elution range and resolution for the
116 selected test compounds. Conditions of pressure and temperature in gradient SFC have been
117 selected to be representative of the conditions the most used in literature, while offering the largest
118 retention range [15, 16].

119 A non-linear density increase and a pressure gradient along the run at fixed BPR pressure (here 140
120 bars) results in a dependency of retention behavior not only to gradient conditions (initial composition,

121 slope) but also to the operating conditions [17, 18]. For any rigorous method transfer of a linear
122 gradient, solute retention should be reported via composition at elution expressed as co-solvent
123 molarity [19, 20]. Nonetheless, for easiness of instrumental setup, the apparent composition at elution
124 (Eq. 1), expressed in volumetric fraction of co-solvent was used throughout this study. This
125 straightforward comparison of elution of analytes is possible, as all experiments were performed on a
126 single instrumentation with highly repeatable pressure profile throughout the runs.

127

128 The composition at elution, C_e , was given by:

$$129 \quad C_e = C_i + \frac{C_f - C_i}{t_g} \times (t_R - t_0 - t_D) \quad (1)$$

130 with t_R the compound retention time and t_D the instrument dwell time.

131 C_i and C_f are the initial and final eluent compositions expressed as volumetric fractions, t_g the gradient
132 time and t_0 the column dead time. The dwell time was determined by performing a triplicate set of
133 gradient profiles without column, with a gradient composition ranging from 60% to 85 % co-solvent. A
134 larger compositional range led to non-linear absorbance profile.

135

136 **3. Results and discussion**

137 This study has been carried out using generic SFC conditions with a gradient elution from 5 % to 50 %
138 co-solvent and a set of neutral, acidic and basic test compounds.

139 Methyl tert-butyl ether (MtBE) is considered as a very weak solvent and the variance generated by the
140 injection in this solvent is considered close to the one generated by heptane, while allowing
141 compounds of a wide range of polarity to be soluble [1]. Hence it was considered through this study as
142 the reference injection solvent. Figure 1 shows the reference chromatogram, with MeOH as co-
143 solvent, when injecting the test compounds diluted in 5 μ L MtBE. The retention times and hence the
144 apparent composition at elution of the test compounds are reported in Table 1. Because of the large
145 dwell volume (1.8 times the column volume), three compounds eluted on the resulting isocratic step, at
146 the initial composition of 5 % MeOH, with retention factor ranging from 0.8 to 1.3. These compounds
147 had a smaller column dispersion contribution and hence were expected to be highly influenced by
148 injection effects, besides instrumental variance. Then the next seven neutral test compounds eluted in
149 the range of 6 % to 35 % MeOH. Retention times were repeatable with intermediate precision (5 days)
150 reaching 2.0 % RSD for the low retained test compounds and 1.3 % RSD for the test compounds
151 eluting during the gradient.

152 Because the viscosity and pressure drop evolved across the gradient, molecular diffusion and hence
153 the column efficiency were not constant through the separation. Efficiency measurements were
154 performed with compounds exhibiting k values around 3, using isocratic composition of either 5 %
155 MeOH or 35 % MeOH and ranged from 17 000 to 9 000 plates, respectively. Hence the peak variance,
156 resulting from the sum of column variance, instrumental variance and injection variance could not be
157 compared from one test compound to another. The individual peak variances σ_{MtBE}^2 were calculated
158 from the reference chromatogram (Figure 1) and were in the range of 300-500 μL^2 (RSD < 10 %) for
159 all test compounds, showing that the instrumental variance ($\leq 37 \mu\text{L}^2$) was negligible under these
160 conditions.

162 **3.1 Adsorption of the injection solvent**

163 Several SFC studies demonstrated that common polar solvents can exhibit retention on polar
164 stationary phases [21, 22]. Detecting at 200 nm so that the MeOH co-solvent exhibited a significant
165 absorbance, it was possible to follow the system peaks due to the elution of solvent molecules.

166 According to the displacement method [23, 24], the injection of a retained solvent produces two zones:
167 the elution zone containing the injected molecules, called “tracer peak” that reflects the retention of the
168 injected molecules, and the displaced elution zone called the “perturbation peak”. The injection of pure
169 MtBE and pure ACN conducted to a single large negative perturbation peak around 0.6 min, while the
170 injection of pure MeOH led to a right angled-triangular perturbation peak, suggesting that MeOH
171 molecules are adsorbed on the stationary phase (Figure 2a). This MeOH adsorption on SFC
172 stationary phases has already been evidenced [22]. The injection of pure ACN provided the exact
173 same elution profile as the injection of MtBE, suggesting that ACN is not retained on the stationary
174 phase. When injecting ACN/water mixtures (Figure 2b), the size and shape of this perturbation peak
175 were not significantly affected by the amount of water. When injecting MeOH/water mixtures (Figure
176 2c), the injected MeOH molecules eluted in the perturbation zone. Increasing the amount of injected
177 MeOH increased the level of UV absorbance in this zone. This suggests that the co-solvent deficiency
178 generated by the injection of ACN/water or MeOH/water migrates at the speed of the MeOH co-
179 solvent, as expected [24].

180
181 By injecting increasing amounts of water, it was also possible to observe a negative peak
182 corresponding to the tracer peak of water, eluting later in the gradient. Figure 2d shows a right
183 angled-triangular shape peak, which area increased with the injected amount of water. Using first-
184 order moment [25], the retention time of this skewed peak was deduced at 2.00 min corresponding to
185 a composition at elution of 13.7 % MeOH co-solvent, proving the large retention of water molecules on
186 DEA stationary phase. Injecting water/ACN mixtures provided a tracer peak with the same retention
187 time and shape, but slightly lower intensity. It is to be noted that during the course of these
188 experiments using 5 μ L sample volume, no difference could be observed on the pressure trace that
189 was highly repeatable whatever the diluent.

190
191 Hence, when injecting samples in hydro-organic phases, both water and methanol molecules from the
192 diluent competed with the analytes for the access to the stationary phase, while ACN molecules had
193 no stationary phase interaction. Hence ACN/water diluents were expected to be less prone to
194 generate injection effects than MeOH/water diluents.

195

196 **3.2 Influence of the diluent composition on peak broadening**

197 Studies on the effect of injection diluents on chromatographic performances have been performed by
198 monitoring column efficiency [11, 22] or peak shapes [1]. However, the first is only applicable on
199 isocratic separation while the latter may not properly reflect focusing/broadening phenomenon. As
200 mentioned before [7], a slight retention shift occurred when increasing the water content in the diluent.

201 The contribution of the composition of the injection solvent to the process of peak broadening can be
202 monitored as the relative variation of peak variance as compared to a similar injection with the sample
203 diluted in MtBE. To more quantitatively describe the effect of the injection solvent on band broadening,
204 the variance generated by the hydro-organic diluent $\sigma_{diluent}^2$ was normalized in regards to the observed
205 variance of the same peak when using MtBE as injection solvent σ_{MtBE}^2 .

206 Figure 3 exhibits the influence of water content in the diluent on the peak broadening. The first
207 observation was that injecting in pure ACN diluent (grey marks) resulted in a larger peak variance for
208 early eluting peaks, as compared to MtBE diluent and as discussed in section 3.1, and had no effect
209 on late-eluting peaks, as expected from a strong solvent effect. On the contrary, when the diluent
210 contained water, the first eluting peaks, with composition at elution lower than 10 %, exhibited a clear
211 compression, i.e. their variance when injected in hydro-organic solvent was lower than when injected
212 in MtBE. For these compounds, the presence of water in the diluent had a clear beneficial effect.
213 Compounds eluting later than the water plug, i.e. with composition at elution higher than 15 % MeOH,
214 encountered a broadening effect. These observations are typical from displacement and tag-along
215 effects when a column is overloaded, here with water molecules. This effect is well documented in
216 preparative liquid chromatography, where the retention of major solutes affects the peak shape of
217 minor solutes [26].

218
219 In analytical SFC, Redei et al. [22] demonstrated that the retention of methanol diluent on an
220 alkylamine column using neat CO₂ as mobile phase conducted to a focusing effect on low retained
221 alkylbenzenes, a broadening effect on alkylbenzenes that were more retained than methanol and that
222 alkylbenzenes that were greatly retained were unaffected by the presence of the diluent. Here we
223 confirmed that the retention of water diluent on the diethylamine stationary phase conducted to a
224 compression of peaks eluting at the initial composition of 5 % MeOH (compounds N1-N3), as soon as
225 10 % water were added to the sample (Figure S1). The compression effect was related to the amount
226 of water. Furthermore, when applying a gradient elution, this compression effect lasted as the amount
227 of co-solvent increased. As shown in Figure 3, the extent of compression was directly linked to the
228 retention of the analyte related to the water retention. The closer the analyte to the water molecules
229 was located, the more compressed the peak was. This compression effect was also related to the
230 amount of water that was injected alongside the low-retained analyte, down to a decrease in peak
231 variance of 40 % when injecting in 90 % water.

232 On the other hand, the tag-along effect that broadened late-eluting peaks seemed to affect more
233 significantly peaks with composition at elution over 30 % co-solvent, with variances reaching + 80 %,
234 whereas for the test compound eluting at a composition of 18 % co-solvent, variance increased only
235 by + 20 %.

236
237 The displacement/tag-along effect is generated by retained molecules that interfere with the retention
238 of analytes. As MeOH was proved to be retained on the SFC column, the dilution of the analytes in a
239 MeOH/water phase had a different impact as when ACN/water was the diluent. For low-retained
240 compounds diluted in over 80 % MeOH, a strong solvent effect was present, due to the competition
241 with the MeOH molecules from the diluent (Figure S2a, black marks) and the compression usually
242 generated by water (Figure S2a, ACN/water diluents, white marks) was annihilated by using MeOH as

243 part of the diluent. The broadening observed for peaks eluting before water, when diluent was 10/90
244 MeOH/water, remains unexplained so far. Because MeOH exhibited a lower retention than water
245 molecules, analyte peaks eluting after water underwent no competition with MeOH diluent molecules
246 and hence their broadening was not significantly affected by the nature of the organic diluent (Figure
247 S2b).

248

249 **3.3 Analyte position relative to water peak**

250 Since the water plug is beneficial for the analytes that migrate faster than water molecules, it may be
251 tempting to modify the chromatographic conditions so that the retention of analytes becomes lower
252 than that of the water. However, the retention of polar compounds in SFC usually follows the same
253 trend and it was necessary to find a stationary phase for which the water retention trend ($\ln k$ vs. co-
254 solvent) intersects with test compounds. Isocratic experiments were performed at co-solvent
255 volumetric fractions ranging from 2 to 40 %, injecting test compounds N6-N9 surrounding the water
256 peak to determine their retention on DEA, diol and HILIC stationary phases (Figure S3). Models
257 expressed as volumetric fractions are easier to use but they are valid only for given operating
258 conditions, here 40 °C, 140 bars at BPR. Any transfer of models would require translation of
259 volumetric fraction into mass fraction of co-solvent [20]. The retention data were fitting a HILIC mixed-
260 mode model for the three columns (Figure S3). The position of test compounds relative to water
261 elution could be switched on HILIC column by changing the gradient slope. At a normalized gradient
262 slope of 2 % (Figure 4a), N9 eluted after water (Ce 12.7 % MeOH vs. 9.3 % MeOH, respectively,
263 calculated using first-order moment), whereas at 30 % normalized gradient slope (Figure 4b), N9
264 eluted before water (27.3 % and Ce 31.1 % MeOH, respectively). The faster elution resulted in an
265 overall peak sharpening (Figure 4) as also observed in LC. For example, for N9 diluted in MtBE, the
266 peak variance decreased from 600 μL^2 to 20 μL^2 for 2 % and 30% normalized gradient slopes,
267 respectively. The effect of water in the diluent was hence normalized for each gradient slope to the
268 variance when the diluent was MtBE. The change of position relative to the water peak confirmed the
269 test compound was compressed if eluting before water molecules, as shown in Figure 4a and
270 broadened if eluting after (figure 4b), with the extent of the phenomenon related to the water content in
271 the diluent.

272

273 **3.4 Influence of the co-solvent nature**

274 Method development in SFC may require the use of different co-solvents to easily tune the separation.
275 Methanol and acetonitrile are the most used co-solvents but mixture of both or ethanol are now
276 gaining attention. As opposed to mobile phase components in LC, SFC co-solvent molecules are
277 known to be prone to interaction with the stationary phase [21, 27]. The impact of the co-solvent
278 nature was studied by comparing variances using MeOH, ACN, mixture of MeOH/ACN 50/50 and
279 EtOH as co-solvent. Changing co-solvents did not affect the retention order of test compounds (Table
280 S1) as polar molecules showed quite similar retention trends in SFC. Solutes injected in MtBE diluent
281 were found to exhibit higher peak variance when the co-solvent was aprotic (ACN) than when it was
282 protic (MeOH or EtOH) (Figure S4a). When the sample was diluted in a water-containing diluent, the
283 trend in variance change was the same as described before, whatever the co-solvent. Solutes that

284 were less retained than water were subjected to two mechanisms: competition with the water diluent
285 leading to peak compression, and competition with the co-solvent molecules to access the stationary
286 phase. For a test compound eluting before water (white marks on Figure 5), it is clear that the
287 competition from alcohol co-solvents (Figures 5a and 5b) was beneficial and the compression
288 increased for peaks closer to water (here, N7). On the contrary, the injection of a water/ACN diluent in
289 an aprotic co-solvent such as ACN (Figure 5c) led to broadening when the content of water was low,
290 and to compression when the content of water in the diluent was elevated.

291 More surprisingly, the use of a mixture of ACN/MeOH 50:50 as a co-solvent, which is expected to
292 generate less competition as less MeOH molecules compete with analytes, was highly compatible with
293 the injection of water/ACN diluents, helping for the compression of early-eluting analyte peaks such as
294 N1. This result has to be mitigated by the fact that MeOH/ACN co-solvent generated much larger
295 peaks than any other co-solvent when injecting samples in apolar diluents (Figure S4a).

296 Finally, because the retention of the studied co-solvent was always lower than water molecules,
297 analyzing compounds with large retention (grey marks in Figure 5) diluted in hydro-organic phases
298 was not affected by the nature of the co-solvent used. Interestingly, Figure 5b suggests that injecting
299 in a water-based diluent led to better results than injecting in MtBE when using an EtOH co-solvent.

300

301 **3.5 Effect of additives in co-solvent**

302 In recent years, water has been introduced as an additive in the organic co-solvent to enhance the
303 mobile phase polarity range [28]. This addition of water, up to 7-8 % with methanol, exhibits a great
304 opportunity for the separation of more polar compounds [29]. Another benefit of adding water to the
305 co-solvent is its impact on peak shapes. Khvalbota et al. [30] reported an improvement in efficiency for
306 neutral compounds isocratically separated on a Fructoshell-N stationary phase, as long as they were
307 more retained than water. Moreover, efficiency was improved for neutral compounds on a silica
308 column, whatever their relative positive towards water.

309 Adding 2 % water in MeOH co-solvent had very little yet positive effects on the gradient separation of
310 neutral test compounds on the DEA stationary phase. Retention was slightly reduced (Table S1).
311 When injection was performed using MtBE, the peak variance was improved for all compounds by 10
312 % - 20 % using water as an additive in co-solvent (Figure S4b). This behavior is similar to what was
313 observed on the silica shell column by Khvaltova [30]. However, the beneficial effect of adding water to
314 the co-solvent was reduced when the sample was also in an aqueous media. As can be seen in Figure
315 6, when comparing the absolute peak variance obtained when using no additive (Figure 6a) or when
316 using water as an additive (Figure 6b), the trend was very similar. Here again, the compounds eluting
317 before the water molecules were compressed, but the influence of the water content in the diluent
318 acted to a lesser extent, the peak variance being already influenced by the water adsorbed on the
319 stationary phase prior to injection. In addition, the tag-along phenomenon was also reduced, with the
320 peak variance increasing by 40 % over the range of diluent composition, compared to 70% when
321 using no additive. This may be due to the fact that the competition between analytes and water for the
322 stationary phase lasted all along the gradient run and not just in the water injection plug. Hence the
323 presence of water in the co-solvent tended to level the effects of water in the diluent, whether
324 beneficial or detrimental.

325

326 In order to introduce an additive that would efficiently compete with the water molecules from the
327 injection solvent, formic acid (FA) was investigated. Anionic additives are often used to improve peak
328 shape when using stationary phases with a basic character such as the Torus DEA [31]. Formic acid
329 can be used in SFC as an alternative to TFA as column regeneration is faster [32]. Formic acid was
330 more retained than water on DEA stationary phase, with a C_e of 23.5 % MeOH. A concentration of 0.1
331 % FA in the methanol co-solvent did not affect the retention of neutral test compounds (Table S1).
332 However, it broadened the peaks significantly for 7 out of 10 compounds using MtBE as diluent
333 (Figure S4b). When comparing the absolute peak variances obtained when injecting in water-
334 containing diluents, the addition of formic acid in the MeOH co-solvent improved the peak variances of
335 retained compounds N8-N10 (Figure 6c), by a factor 30 % - 50 % compared to the use of pure MeOH
336 as co-solvent, while it had a dramatic effect on less retained compounds N4-N7 with absolute peak
337 variances increasing by a factor 3. Hence, formic acid as an additive to MeOH has to be avoided if
338 MtBE is the sample diluent. Nonetheless it may be of interest for highly polar solutes diluted in
339 ACN/water.

340

341 **3.6 Ionizable solutes**

342 The expansion of SFC applications towards more polar compounds such as metabolites, amino acids,
343 nucleoside, peptides [2] pave the road towards the analysis of ionized molecules by LC x SFC. These
344 highly polar analytes typically elute from LC in a great amount of water thus it seemed essential to
345 check the behavior of ionized test compounds in this study.

346 West et al. stated using pH indicator that the apparent aqueous pH of carbon dioxide – methanol
347 compositions should be around pH 5 with a decreased value when the proportion of methanol
348 increased [33]. The selected acidic test compounds (pK_a around 4.5) were supposed to be partially
349 ionized. Interestingly, the peak variance of acidic compounds was not influenced by the content of
350 water in the diluent (Figure 7).

351 With composition at elution over 20 % MeOH, the selected acidic test compounds A1-A3 were highly
352 retained. However, no peak broadening was observed on these negative analytes, whatever the
353 content of water in the diluent while neutral compounds eluting at the same composition (N4 and N8)
354 suffered an increase in peak width which extent was linked to the water content in the diluent, as
355 previously discussed.

356 On the other hand, two basic test compounds B1 and B2 were analyzed, B1 with a lower retention
357 than water, and B2 with a larger retention than water. Ammonium hydroxide was added to the co-
358 solvent to improve peak symmetry [14]. Selected test compounds had both a pK_a at 9.4 and so the
359 assumption can be made that they were fully protonated all along the gradient run. Unlike for other test
360 compounds, MtBE as an injection solvent was found to provide symmetrical yet very wide peaks.
361 Hence a mixture of ACN/water 90:10 was used as the injection solvent of reference for the calculation
362 of variance change. The general trend for basic solutes followed what was observed for neutral
363 solutes, with a peak compression for compounds eluting before the water peak and an increase in
364 peak width for compounds more retained than water (Figure 7b). The compression on low-retained B1
365 peak ranged between -5 % and - 20 % depending on the water content, which was very close to the
366 value observed for the neutral test compound N4 eluting at the same composition. On the other hand,
367 the selected retained basic compound B2 eluted at C_e 15 % MeOH which was very close to the water

368 peak. The increase in peak width that B2 underwent was of a much larger extent than the one
369 observed for the neutral test compound N8 eluting at its vicinity.

370
371 While these results need to be confirmed with a much larger pool of ionizable compounds, it seems
372 that in the case of our selected test compounds, negatively charged solutes and positively charged
373 solutes exhibiting a lower retention than water molecules were not influenced by the water content in
374 the injection solvent. On the contrary, the presence of water-rich solvent was detrimental for the
375 positively-charged compounds with a retention close to water.

376
377 Adding 2 % water to the co-solvent was positive for the peak shapes of basic compounds when the
378 injection solvent was of low polarity such as MtBE, as previously stated by West and Lemasson [34],
379 but it was found highly detrimental when injecting in a water-based phase (Figure S5a). Injecting water
380 in a water-containing co-solvent led to the formation of a perturbation peak at 2.5 min and a tracer
381 peak at 3.4 min, visible at 200 nm (Figure S5b). With water content as low as 10 % in the diluent, the
382 peaks of basic compounds eluting before the perturbation peak were splitting towards higher retention.
383 The peaks with higher retention kept symmetrical shape up to 30 % water in the diluent, then when
384 increasing the amount of water in the diluent, the peaks also splitted towards higher retention. In
385 comparison, acidic or neutral compounds never underwent any splitting in the same conditions.

386

387 **3.7 Increasing the injection volume**

388 Desfontaines et al. [1] stated that injection of samples with high content of water was possible for low
389 injection volume ($< 2 \mu\text{L}$) while the injection of $10 \mu\text{L}$ (2 % column volume) conducted to a demixing
390 when using an initial mobile phase containing only 2 % co-solvent (MeOH/water 98:2 + 0.1 %
391 ammonium hydroxide). The solubility of water is indeed very low in supercritical CO_2 ($\sim 0.1\%$ w/w).
392 Increasing the initial mobile phase composition to 5 % MeOH increased the solubility of water and
393 during the course of our experiments, a volume of $10 \mu\text{L}$ of a sample diluted in pure water could be
394 injected on a column of similar geometry ($100 \times 3.0 \text{ mm}$, $1.7 \mu\text{m}$) without demixing issue. Increasing
395 the injection volume from $5 \mu\text{L}$ to $10 \mu\text{L}$ led to an expected peak broadening but the peaks remained
396 symmetrical, and retention times and system pressure kept unchanged. The peak capacity when
397 injecting in water-containing diluents remained above 75 % of the peak capacity observed when
398 injecting $10 \mu\text{L}$ sample in MtBE. Increasing the injection volume to $20 \mu\text{L}$ (4 % column volume) led to
399 two increases in the profile of the system pressure (Figure S6a). The first one occurred during the
400 elution of MeOH molecules while the second one occurred during the elution of water molecules.
401 Since both increases were proportional to the amount of water injected in the column, we suggest they
402 were due to the local increase of viscosity generated by 1) the displaced MeOH molecules and 2) the
403 water plug. Pressure values were back to normal as soon as water eluted out of the column. While
404 peaks were broadening and splitting with an increase content of water in the diluent, injecting 90%
405 water diluent led to a massively distorted broad peak for compounds eluting at the vicinity of water
406 molecules (Figure 8). However, the system peak due to water was visible at the same time at it was
407 when injecting $5 \mu\text{L}$ (Figure S6b) and the UV signal was not disrupted, suggesting that water plug still
408 eluted at the same velocity and demixing was not happening. A better understanding of water

409 interaction with stationary phase and solutes in SFC would be required before injecting such amount
410 of water diluent.

411 On the other hand, neutral test compounds eluting at the end of the gradient, such as N10, exhibited
412 fronting peaks while peaks from acidic test compounds with the same retention time remained
413 symmetrical with no retention shift (Figure 8). Supposedly, ionic interactions with the stationary phase
414 in SFC played a role in maintaining the peak symmetry for acidic test compounds in this study, but this
415 point needs a deeper investigation with a larger set of ionizable compounds.

416

417 **4. Conclusion**

418 The composition of the sample diluent has a major role in the peak broadening in SFC. While previous
419 papers highlighted the strong solvent effect due to polar solvents such as alcohols, this work focuses
420 on the injection of water-based diluents. Peak broadening of 10 test compounds were compared when
421 injected either in MtBE or in diluents containing up to 90 % water. Statements that water has a
422 negative effect on peak shape when it is part of the diluent is only partly true. When injected
423 simultaneously with neutral analytes, water plays a competing role for the SFC stationary phase,
424 leading to a compression of peaks that elute before water, and a broadening of peaks that elute after
425 water. The phenomenon is related to 1) the retention of analytes in regards to the retention of water
426 and 2) the amount of water in the diluent. It has been confirmed on various stationary phases. Adding
427 water or acidic additive to the co-solvent did not affect this process for neutral analytes. The presence
428 of water along acidic analytes in the sample had no effect on their peak shapes, while for basic
429 compounds, it led to dramatic peak deformation. Moreover it was possible to inject 10 μL of samples in
430 water-containing diluents (2 % column volume) without major peak capacity loss, while increasing the
431 injection volume up to 20 μL had negative consequences on peak shapes of neutral molecules. In the
432 light of these results, the analysis of polar compounds diluted in hydro-organic mixtures, or the use of
433 SFC as second dimension in a two-dimensional separation of neutral compounds could be considered
434 without requiring sample water removal, providing that injection volume remained below 2 % of the
435 column volume. Interestingly, acidic compounds can hold very large injection volumes with water-rich
436 diluents, while the analysis of basic compounds seems problematic even at very small injection
437 volume. While this study highlighted clear trends for neutral compounds, a deeper investigation will be
438 required for ionizable compounds.

439

440 **5. Acknowledgments**

441 The authors are deeply grateful to Agilent Technologies for the loan of the Infinity I fixed-loop injection
442 module and especially Audrey Menet for her technical advices. Marion Bulet-Parendel is
443 acknowledged for preliminary results.

444

445 **6. References**

- 447 [1] V. Desfontaine, A. Tarafder, J. Hill, J. Fairchild, A. Grand-Guillaume Perrenoud, J.-L. Veuthey, D.
448 Guillaume, A systematic investigation of sample diluents in modern supercritical fluid chromatography,
449 *Journal of Chromatography A* 1511 (2017) 122-131 <https://doi.org/10.1016/j.chroma.2017.06.075>.
- 450 [2] G.L. Losacco, J.-L. Veuthey, D. Guillaume, Metamorphosis of supercritical fluid chromatography: A
451 viable tool for the analysis of polar compounds?, *TrAC Trends in Analytical Chemistry* 141 (2021)
452 116304 <https://doi.org/10.1016/j.trac.2021.116304>.
- 453 [3] M. Burlet-Parendel, K. Faure, Opportunities and challenges of liquid chromatography coupled to
454 supercritical fluid chromatography, *TrAC Trends in Analytical Chemistry* 144 (2021) 116422
455 <https://doi.org/10.1016/j.trac.2021.116422>.
- 456 [4] A.S. Kaplitz, M.E. Mostafa, S.A. Calvez, J.L. Edwards, J.P. Grinias, Two-dimensional separation
457 techniques using supercritical fluid chromatography, *Journal of Separation Science* 44 (2021) 426-437
458 <https://doi.org/10.1002/jssc.202000823>.
- 459 [5] M. Enmark, D. Åsberg, A. Shalliker, J. Samuelsson, T. Fornstedt, A closer study of peak distortions
460 in supercritical fluid chromatography as generated by the injection, *Journal of Chromatography A* 1400
461 (2015) 131-139 <https://doi.org/10.1016/j.chroma.2015.04.059>.
- 462 [6] K. Vanderlinden, G. Desmet, K. Broeckhoven, Effect of the feed injection method on band
463 broadening in analytical supercritical fluid chromatography, *Journal of Chromatography A* 1630 (2020)
464 461525 <https://doi.org/10.1016/j.chroma.2020.461525>.
- 465 [7] M. Sarrut, A. Corgier, G. Cretier, A. Le Masle, S. Dubant, S. Heinisch, Potential and limitations of
466 on-line comprehensive reversed phase liquid chromatography x supercritical fluid chromatography for
467 the separation of neutral compounds: An approach to separate an aqueous extract of bio-oil, *Journal*
468 *of Chromatography A* 1402 (2015) 124-133 [10.1016/j.chroma.2015.05.005](https://doi.org/10.1016/j.chroma.2015.05.005).
- 469 [8] M. Sun, M. Sandahl, C. Turner, Comprehensive on-line two-dimensional liquid
470 chromatography x supercritical fluid chromatography with trapping column-assisted modulation for
471 depolymerised lignin analysis, *Journal of Chromatography A* 1541 (2018) 21-30
472 <https://doi.org/10.1016/j.chroma.2018.02.008>.
- 473 [9] C.J. Venkatramani, M. Al-Sayah, G. Li, M. Goel, J. Girotti, L. Zang, L. Wigman, P. Yehl, N.
474 Chetwyn, Simultaneous achiral-chiral analysis of pharmaceutical compounds using two-dimensional
475 reversed phase liquid chromatography-supercritical fluid chromatography, *Talanta* 148 (2016) 548-555
476 <https://doi.org/10.1016/j.talanta.2015.10.054>.
- 477 [10] M. Goel, E. Larson, C.J. Venkatramani, M.A. Al-Sayah, Optimization of a two-dimensional liquid
478 chromatography-supercritical fluid chromatography-mass spectrometry (2D-LC-SFC-MS) system to
479 assess "in-vivo" inter-conversion of chiral drug molecules, *Journal of Chromatography B* 1084 (2018)
480 89-95 <https://doi.org/10.1016/j.jchromb.2018.03.029>.
- 481 [11] R. De Pauw, K. Shoykhet, G. Desmet, K. Broeckhoven, Understanding and diminishing the extra-
482 column band broadening effects in supercritical fluid chromatography, *Journal of Chromatography A*
483 1403 (2015) 132-137 <https://doi.org/10.1016/j.chroma.2015.05.017>.
- 484 [12] M. Enmark, E. Glenne, M. Leško, A. Langborg Weinmann, T. Leek, K. Kaczmarski, M. Klarqvist,
485 J. Samuelsson, T. Fornstedt, Investigation of robustness for supercritical fluid chromatography
486 separation of peptides: Isocratic vs gradient mode, *Journal of Chromatography A* 1568 (2018) 177-187
487 <https://doi.org/10.1016/j.chroma.2018.07.029>.
- 488 [13] C. West, Current trends in supercritical fluid chromatography, *Analytical and Bioanalytical*
489 *Chemistry* 410(25) (2018) 6441-6457 [10.1007/s00216-018-1267-4](https://doi.org/10.1007/s00216-018-1267-4).
- 490 [14] A. Grand-Guillaume Perrenoud, J.-L. Veuthey, D. Guillaume, Comparison of ultra-high
491 performance supercritical fluid chromatography and ultra-high performance liquid chromatography for
492 the analysis of pharmaceutical compounds, *Journal of Chromatography A* 1266 (2012) 158-167
493 <https://doi.org/10.1016/j.chroma.2012.10.005>.
- 494 [15] M.A. Khalikova, E. Lesellier, E. Chapuzet, D. Šatinský, C. West, Development and validation of
495 ultra-high performance supercritical fluid chromatography method for quantitative determination of nine
496 sunscreens in cosmetic samples, *Analytica Chimica Acta* 1034 (2018) 184-194
497 <https://doi.org/10.1016/j.aca.2018.06.013>.
- 498 [16] Y. Huang, T. Zhang, Y. Zhao, H. Zhou, G. Tang, M. Fillet, J. Crommen, Z. Jiang, Simultaneous
499 analysis of nucleobases, nucleosides and ginsenosides in ginseng extracts using supercritical fluid
500 chromatography coupled with single quadrupole mass spectrometry, *Journal of Pharmaceutical and*
501 *Biomedical Analysis* 144 (2017) 213-219 <https://doi.org/10.1016/j.jpba.2017.03.059>.
- 502 [17] R. De Pauw, K. Shoykhet, G. Desmet, K. Broeckhoven, Effect of reference conditions on flow
503 rate, modifier fraction and retention in supercritical fluid chromatography, *Journal of Chromatography*
504 *A* 1459 (2016) 129-135 <https://doi.org/10.1016/j.chroma.2016.06.040>.
- 505 [18] G. Guiochon, A. Tarafder, Fundamental challenges and opportunities for preparative supercritical
506 fluid chromatography, *Journal of Chromatography A* 1218(8) (2011) 1037-1114
507 <https://doi.org/10.1016/j.chroma.2010.12.047>.

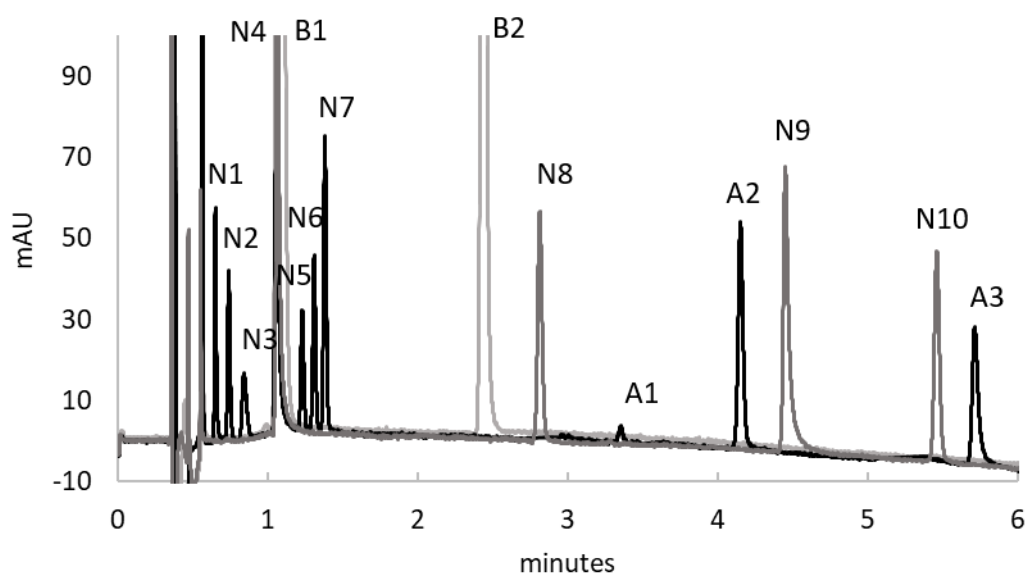
508 [19] E. Glenne, H. Leek, M. Klarqvist, J. Samuelsson, T. Fornstedt, Systematic investigations of peak
509 deformations due to co-solvent adsorption in preparative supercritical fluid chromatography, *Journal of*
510 *Chromatography A* 1496 (2017) 141-149 <https://doi.org/10.1016/j.chroma.2017.03.053>.
511 [20] M. Enmark, J. Samuelsson, T. Fornstedt, A Retention-Matching Strategy for Method Transfer in
512 Supercritical Fluid Chromatography: Introducing the Isomolar Plot Approach, *Analytical Chemistry*
513 93(16) (2021) 6385-6393 10.1021/acs.analchem.0c05142.
514 [21] E. Glenne, K. Öhlén, H. Leek, M. Klarqvist, J. Samuelsson, T. Fornstedt, A closer study of
515 methanol adsorption and its impact on solute retentions in supercritical fluid chromatography, *Journal*
516 *of Chromatography A* 1442 (2016) 129-139 <https://doi.org/10.1016/j.chroma.2016.03.006>.
517 [22] C. Rédei, A. Felinger, Modeling the competitive adsorption of sample solvent and solute in
518 supercritical fluid chromatography, *Journal of Chromatography A* 1603 (2019) 348-354
519 <https://doi.org/10.1016/j.chroma.2019.05.045>.
520 [23] P. Forssén, J. Lindholm, T. Fornstedt, Theoretical and experimental study of binary perturbation
521 peaks with focus on peculiar retention behaviour and vanishing peaks in chiral liquid chromatography,
522 *Journal of Chromatography A* 991(1) (2003) 31-45 [https://doi.org/10.1016/S0021-9673\(03\)00213-9](https://doi.org/10.1016/S0021-9673(03)00213-9).
523 [24] T. Fornstedt, P. Forssén, D. Westerlund, System peaks and their impact in liquid chromatography,
524 *TrAC Trends in Analytical Chemistry* 81 (2016) 42-50 <https://doi.org/10.1016/j.trac.2016.01.008>.
525 [25] J.P. Foley, J.G. Dorsey, Equations for Calculation of Chromatographic Figures of Merit for Ideal
526 and Skewed Peaks, *Anal. Chem.* 83(55) (1983) 730-737
527 [26] S. Golshan-Shirazi, G. Guiochon, Theoretical explanation of the displacement and tag-along
528 effects, *Chromatographia* 30(11) (1990) 613-617 10.1007/BF02269733.
529 [27] P. Vajda, G. Guiochon, Modifier adsorption in supercritical fluid chromatography onto silica
530 surface, *Journal of Chromatography A* 1305 (2013) 293-299
531 <https://doi.org/10.1016/j.chroma.2013.06.075>.
532 [28] D. Roy, A. Tarafder, L. Miller, Effect of water addition to super/sub-critical fluid mobile-phases for
533 achiral and chiral separations, *TrAC Trends in Analytical Chemistry* 145 (2021) 116464
534 <https://doi.org/10.1016/j.trac.2021.116464>.
535 [29] G.L. Losacco, O. Ismail, J. Pezzatti, V. González-Ruiz, J. Boccard, S. Rudaz, J.-L. Veuthey, D.
536 Guillaume, Applicability of Supercritical fluid chromatography–Mass spectrometry to metabolomics. II–
537 Assessment of a comprehensive library of metabolites and evaluation of biological matrices, *Journal of*
538 *Chromatography A* 1620 (2020) 461021 <https://doi.org/10.1016/j.chroma.2020.461021>.
539 [30] L. Khvalbota, D. Roy, M.F. Wahab, S.K. Firooz, A. Machyňáková, I. Špánik, D.W. Armstrong,
540 Enhancing supercritical fluid chromatographic efficiency: Predicting effects of small aqueous additives,
541 *Analytica Chimica Acta* 1120 (2020) 75-84 <https://doi.org/10.1016/j.aca.2020.04.065>.
542 [31] G.L. Losacco, J.O. DaSilva, J. Liu, E.L. Regalado, J.-L. Veuthey, D. Guillaume, Expanding the
543 range of sub/supercritical fluid chromatography: Advantageous use of methanesulfonic acid in water-
544 rich modifiers for peptide analysis, *Journal of Chromatography A* 1642 (2021) 462048
545 <https://doi.org/10.1016/j.chroma.2021.462048>.
546 [32] C. Brunelli, Y. Zhao, M.-H. Brown, P. Sandra, Pharmaceutical analysis by supercritical fluid
547 chromatography: Optimization of the mobile phase composition on a 2-ethylpyridine column, *Journal*
548 *of Separation Science* 31(8) (2008) 1299-1306 <https://doi.org/10.1002/jssc.200700555>.
549 [33] C. West, J. Melin, H. Ansouri, M. Mengue Metogo, Unravelling the effects of mobile phase
550 additives in supercritical fluid chromatography. Part I: Polarity and acidity of the mobile phase, *Journal*
551 *of Chromatography A* 1492 (2017) 136-143 <https://doi.org/10.1016/j.chroma.2017.02.066>.
552 [34] C. West, E. Lemasson, Unravelling the effects of mobile phase additives in supercritical fluid
553 chromatography—Part II: Adsorption on the stationary phase, *Journal of Chromatography A* 1593
554 (2019) 135-146 <https://doi.org/10.1016/j.chroma.2019.02.002>.
555

556
557
558
559
560

Table 1: Selected **test compounds** and associated retention time and composition at elution **using DEA column**. MeOH as co-solvent for neutral and acidic compounds, **MeOH + 2 % water + 20 mM ammonium hydroxide for basic compounds**.

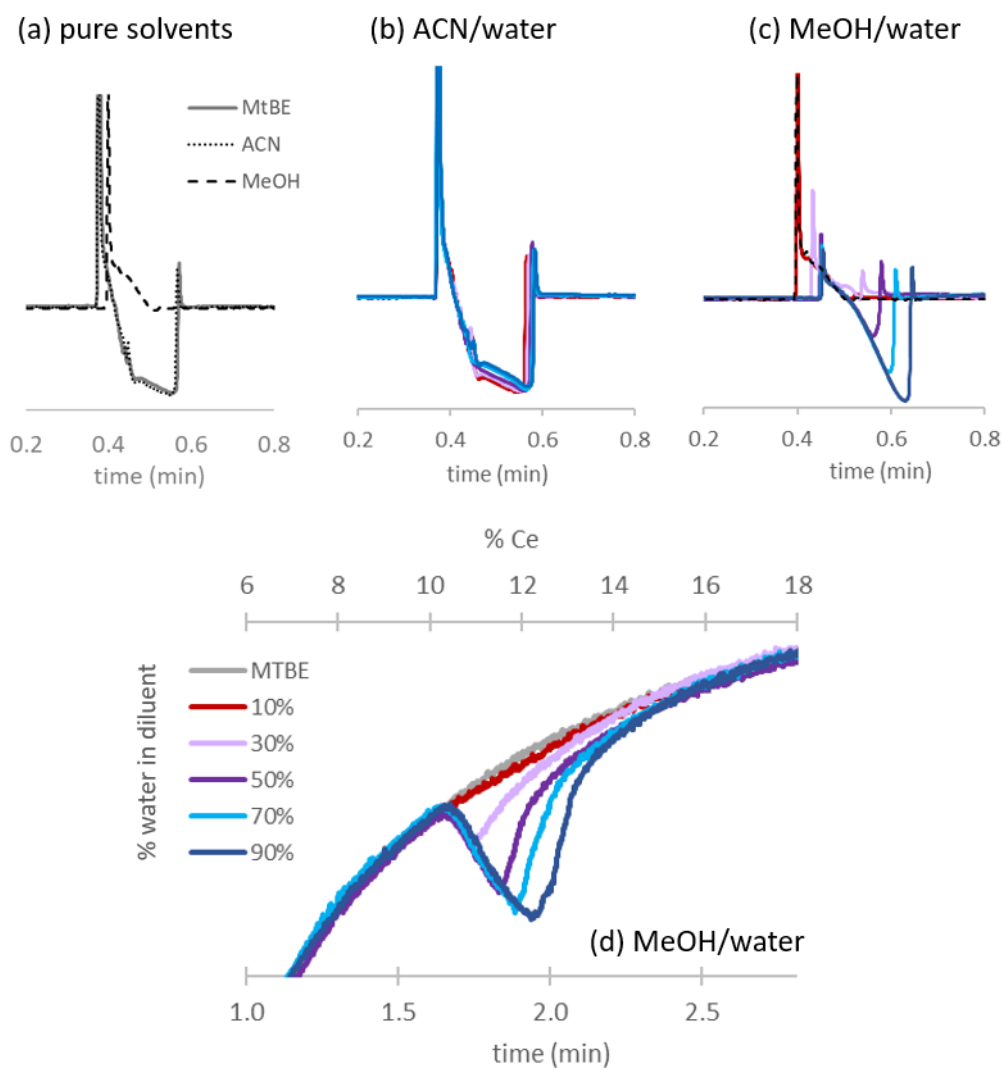
	Probe number	log P	tr (min)	Ce (%)	
Neutral	eugenol	N1	2.223	0.65	5.0
	2.4.6 trimethylphenol	N2	1.7	0.74	5.0
	1-indanol	N3	1.518	0.84	5.0
	apocynin	N4	0.77	1.05	6.3
	o-cresol	N5	1.95	1.23	7.5
	m-cresol	N6	1.96	1.31	8.0
	phenol	N7	1.46	1.38	8.5
	4-hydroxybenzyl alcohol	N8	-0.121	2.81	17.9
	naringenin	N9	0.79	4.45	28.7
	arbutin	N10	-0.652	5.45	35.3
Acidic	acrylic acid	A1	0.35	3.35	21.4
	trans cinnamic acid	A2	1.887	4.15	26.7
	ferulic acid	A3	0.78	5.71	37.0
Basic	imipramine	B1	3.112	1.08	6.4
	propranolol	B2	2.535	2.44	15.4

561
562
563

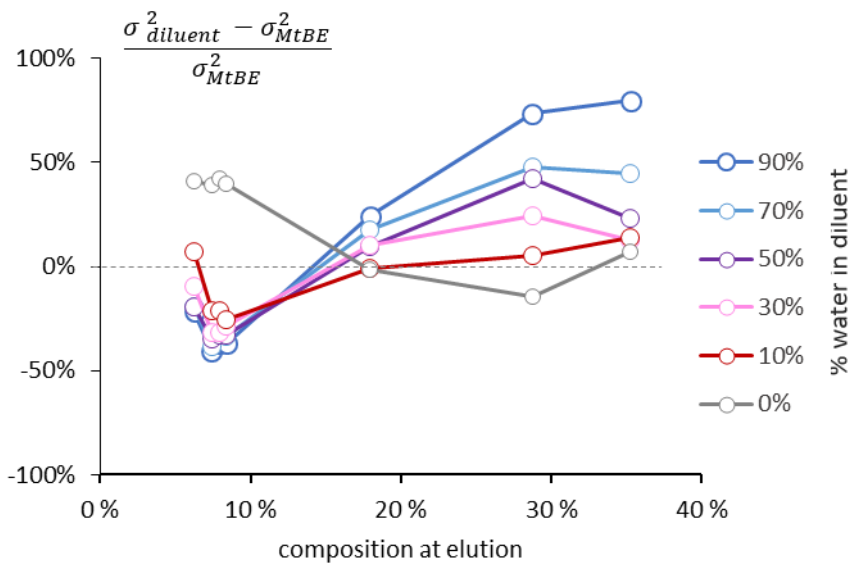


564
 565
 566
 567
 568
 569
 570

Figure 1: Separation of the 15 test compounds. Column DEA. Co-solvent MeOH for neutral and acidic compounds (N1-N10; A1-A3) and co-solvent MeOH + 2 % water + 20 mM ammonium hydroxide for basic compounds (B1-B2). Injection 5 μ L in MtBE diluent. Detection 220 nm. Test compounds description: refer to table 1.

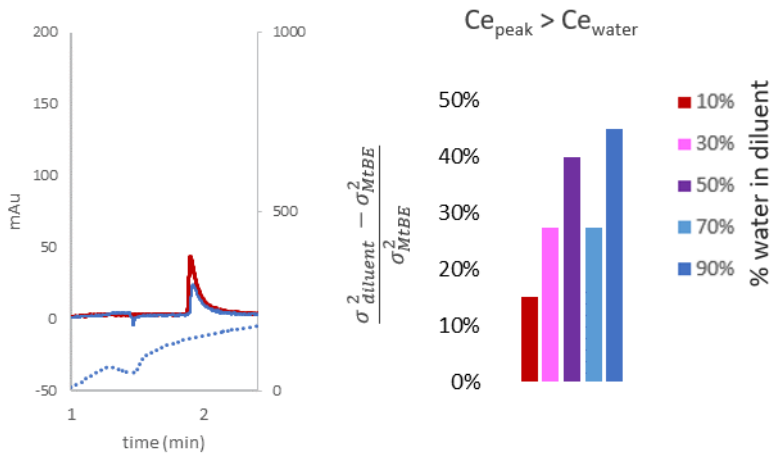


571
 572
 573 Figure 2: Chromatograms corresponding to the injection of (a) pure diluents: MtBE (grey line), ACN
 574 (dotted line) and MeOH (dashed line), (b) ACN/water mixtures and (c, d) MeOH/water mixtures. The
 575 colored lines correspond to increasing amounts of water in diluent, from 10 % (red line) to 90 % (blue
 576 line). Column DEA. Co-solvent MeOH. Injection volume 5 μ L. Detection at 200 nm.
 577

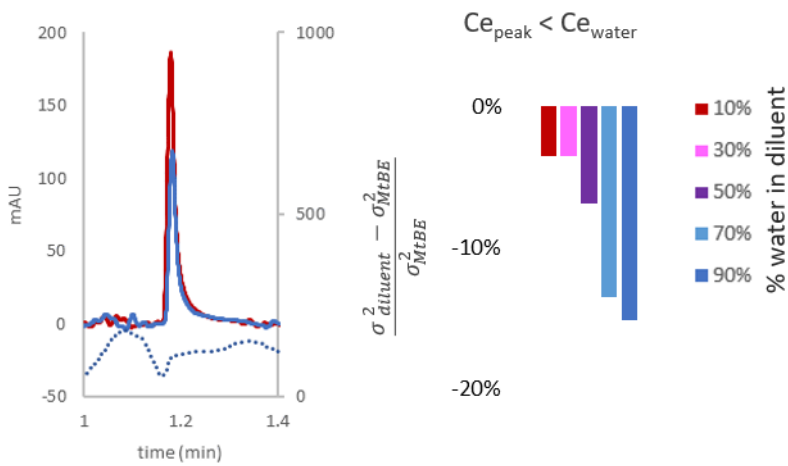


578
 579 Figure 3: Diluent effect reported as change in peak variance vs. the composition at elution of neutral
 580 test compounds, for various percentages of water in the ACN: water diluent. Reference variance from
 581 the injection of test compounds using MtBE as diluent, with conditions as in Figure 1.
 582
 583

(a) normalized gradient slope 2 %



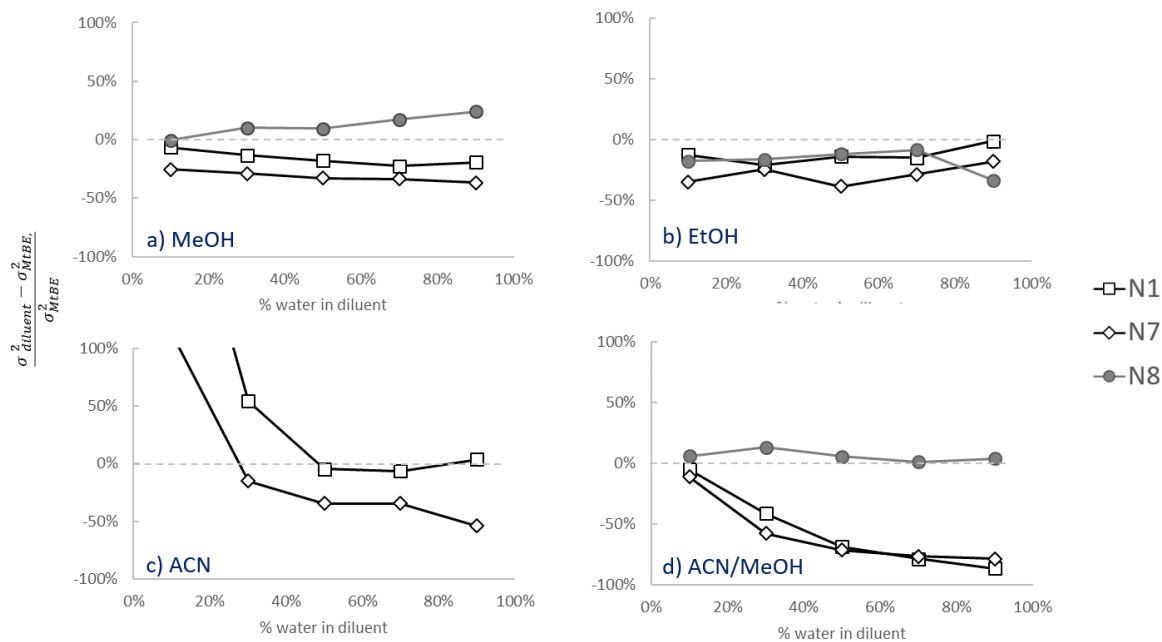
(b) normalized gradient slope 30 %



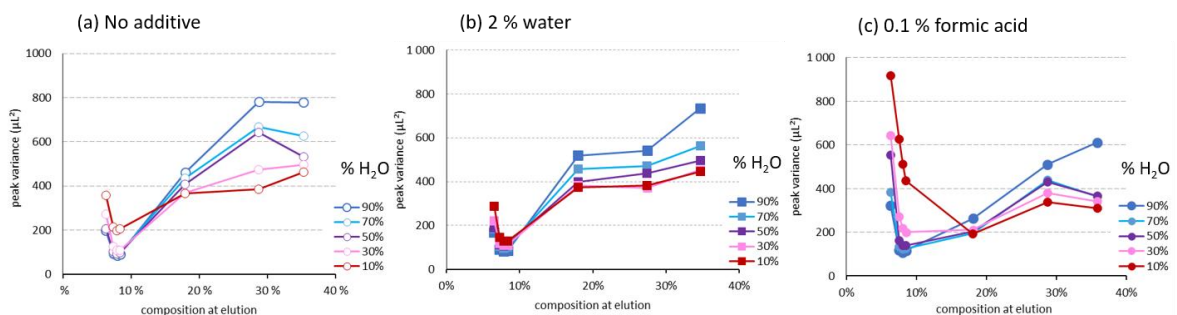
584

585 Figure 4: Chromatograms of N9 (plain line, 220 nm) and water (dashed line, 200 nm) and associated
 586 injection solvent effects, for a) a normalized gradient slope of 2 % and b) a normalized gradient slope
 587 of 30 %. HILIC column, gradient 5 % to 40 % MeOH.

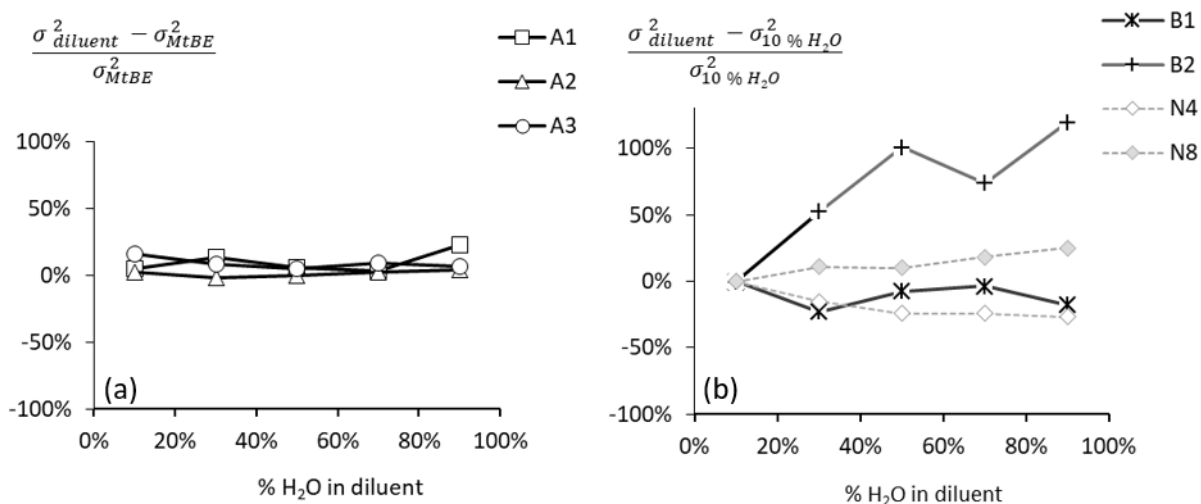
588



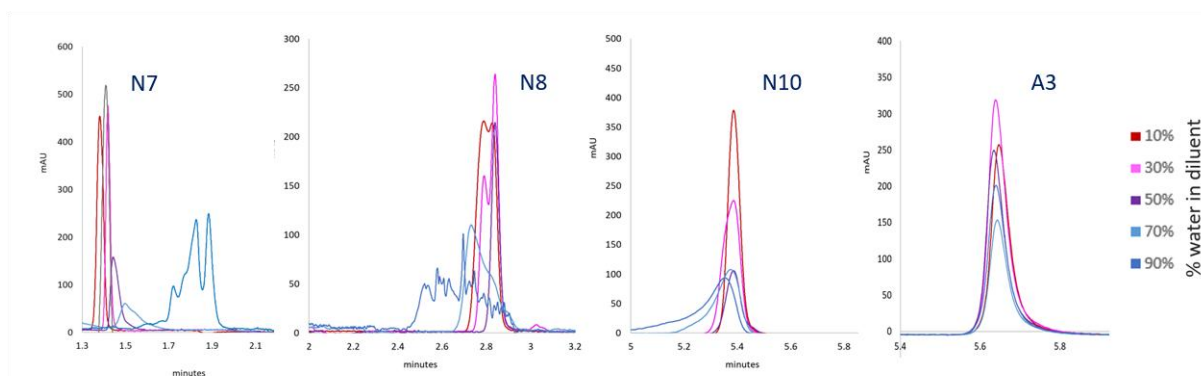
589
 590 Figure 5: Influence of the co-solvent on the change in peak variance vs. the content of water in the
 591 ACN/H₂O diluent, for co-solvent (a) MeOH, (b) ACN, (c) EtOH and (d) MeOH/ACN 50/50. Compounds
 592 N1-N7 (black marks) elute before water, N8 (grey marks) after water. Please refer to Table S1 for the
 593 values of composition at elution in the different co-solvents.
 594



595
 596 Figure 6: Effect of additives in modifier on the peak variance for various water content in the
 597 ACN/water diluent. Mobile phase CO₂ with the co-solvent (a) MeOH, (b) MeOH +2 % v/v water and (c)
 598 MeOH + 0.1 % w/w formic acid
 599



600
 601 Figure 7: Diluent effect reported as change in peak variance vs. the content of water in the diluent. (a)
 602 acidic test compounds A1-A3, with MtBE diluent as reference and (b) basic test compounds B1-B2
 603 with ACN/water 90:10 diluent as reference. The dashed lines represent test compounds N4 (white
 604 diamond) and N8 (grey diamond).
 605



606
 607 Figure 8. Chromatograms of three neutral probes and one acidic probe. Injection 20 μ L. Column DEA.
 608 Co-solvent MeOH. UV detection 220 nm. Other conditions as stated in the text.
 609

610
611
612
613
614
615
616
617
618
619
620
621
622
623
624
625
626
627
628
629
630
631
632
633
634
635
636
637
638
639
640
641
642
643
644
645
646
647
648
649
650

Supplementary material

Effect of the injection of water-containing diluents on band broadening in analytical supercritical fluid chromatography

Magali Batteau¹, Karine Faure¹

¹Université de Lyon, CNRS, Université Claude Bernard Lyon 1, Institut des Sciences Analytiques, UMR 5280, 5 rue de la Doua, F-69100 VILLEURBANNE, France

*Corresponding author: karine.faure@isa-lyon.fr

List of supplementary material

Figure S1: Change in peak variance for peaks N1-N3 eluting at initial mobile phase composition, for various percentages of water in the ACN/water diluent. Column DEA, co-solvent MeOH.

Figure S2: Injection solvent effect reported as change in peak variance for (a) N6 and (b) N10 vs. the content of water in the diluent, the remaining solvent being acetonitrile (white marks) or methanol (black marks).

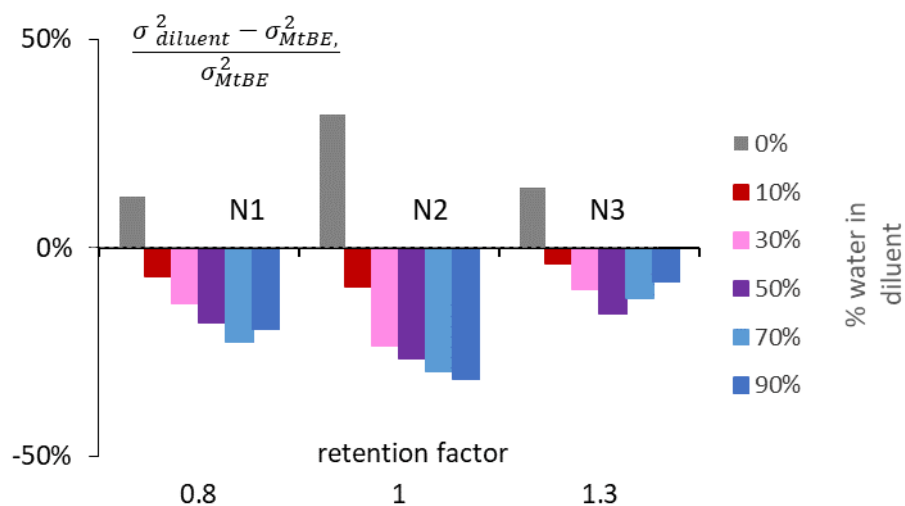
Figure S3: Retention relationships of water and four surrounding probes N6-N9. $\ln k$ as a function of the MeOH content in mobile phase. Circles are experimental measurements based on isocratic runs. Plain lines are the associated prediction using mixed-mode model. Below are the associated prediction errors of three models. Percentage errors defined as $(k_{\text{predicted}} - k_{\text{exp}})/k_{\text{exp}}$. Columns (a) Torus DEA, (b) Torus diol and (c) BEH HILIC.

Figure S4: Peak variance of the neutral test compounds, using MtBE as diluent, (a) for various organic co-solvents and (b) using MeOH with additives, i.e. 2 % water or 0.1 % formic acid additives as co-solvent. Compounds N8-N10 were not eluting during the gradient when using ACN as co-solvent.

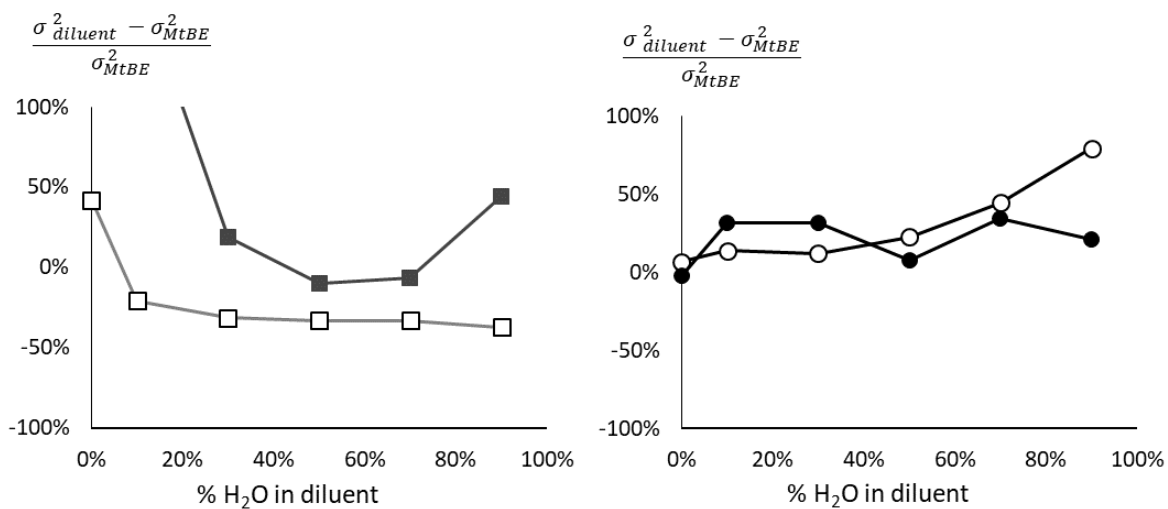
Figure S5: (a) Chromatograms of two basic probes injected in ACN/water diluent with increasing content of water. UV detection 220 nm. (b) UV trace of pure water. UV detection 200 nm. Column DEA. Co-solvent MeOH + 2 % water + 20 mM ammonium hydroxide.

Figure S6: a) SFC inlet pressure when injecting 20 μL ACN/water with increasing content of water and b) System peaks recorded at 200 nm, when injecting 5 μL and 20 μL pure water. Column DEA. Co-solvent MeOH. Other conditions stated in text.

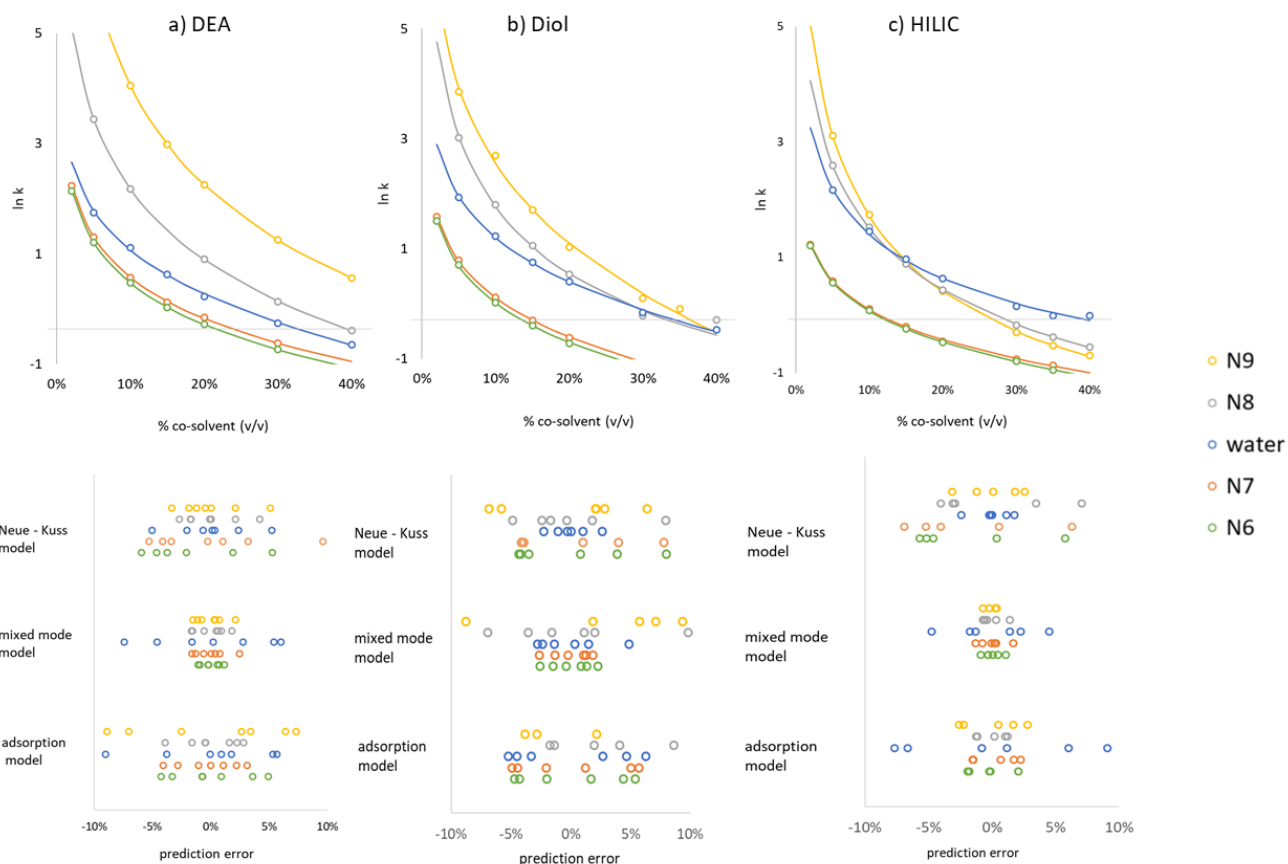
Table S1: Selected test compounds and associated composition at elution for different co-solvents. Column DEA, gradient 5 % to 50 % co-solvent, normalized gradient slope 2 %.



651
 652 Figure S1: Change in peak variance for peaks N1-N3 eluting at initial mobile phase composition, for
 653 various percentages of water in the ACN/ water diluent. Column DEA, co-solvent MeOH.
 654
 655
 656
 657
 658



659
 660 Figure S2: Injection solvent effect reported as change in peak variance for (a) N6 and (b) N10 vs. the
 661 content of water in the diluent, the remaining solvent being acetonitrile (white marks) or methanol
 662 (black marks).
 663



664
665

666 Figure S3: Retention relationships of water and four surrounding probes N6-N9. Ln k as a function of
 667 the MeOH content in mobile phase. Circles are experimental measurements based on isocratic runs.
 668 Plain lines are the associated prediction using mixed-mode model. Below are the associated
 669 prediction errors of three models. Percentage errors defined as $(k_{\text{predicted}} - k_{\text{exp}})/k_{\text{exp}}$. Columns (a)
 670 Torus DEA, (b) Torus diol and (c) BEH HILIC.

671
672

673 **Equations for**

674 Neue-Kuss model $\ln k = \ln k_0 + 2 \ln(1 + S_2 \phi) - \frac{S_1 \phi}{1 + S_2 \phi}$

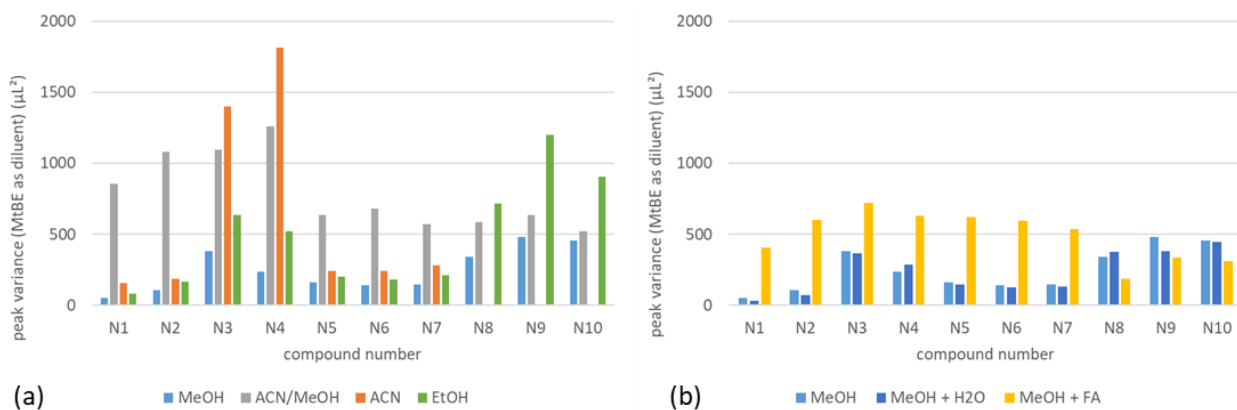
675 Mixed-mode model $\ln k = \ln k_0 + S_1 \phi + S_2 \ln \phi$

676 Adsorption model $\ln k = \ln k_0 - S_1 \ln \phi$

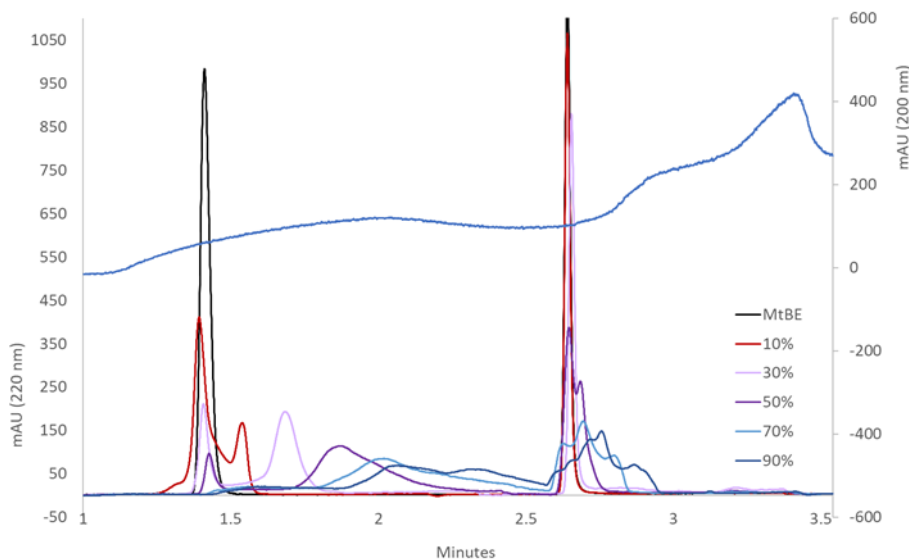
677

678 where ϕ is the volumetric fraction of co-solvent, k_0 the extrapolated value of k for $\phi = 0$ (i.e., pure CO₂),
 679 S1 the slope and S2 the curvature coefficient.

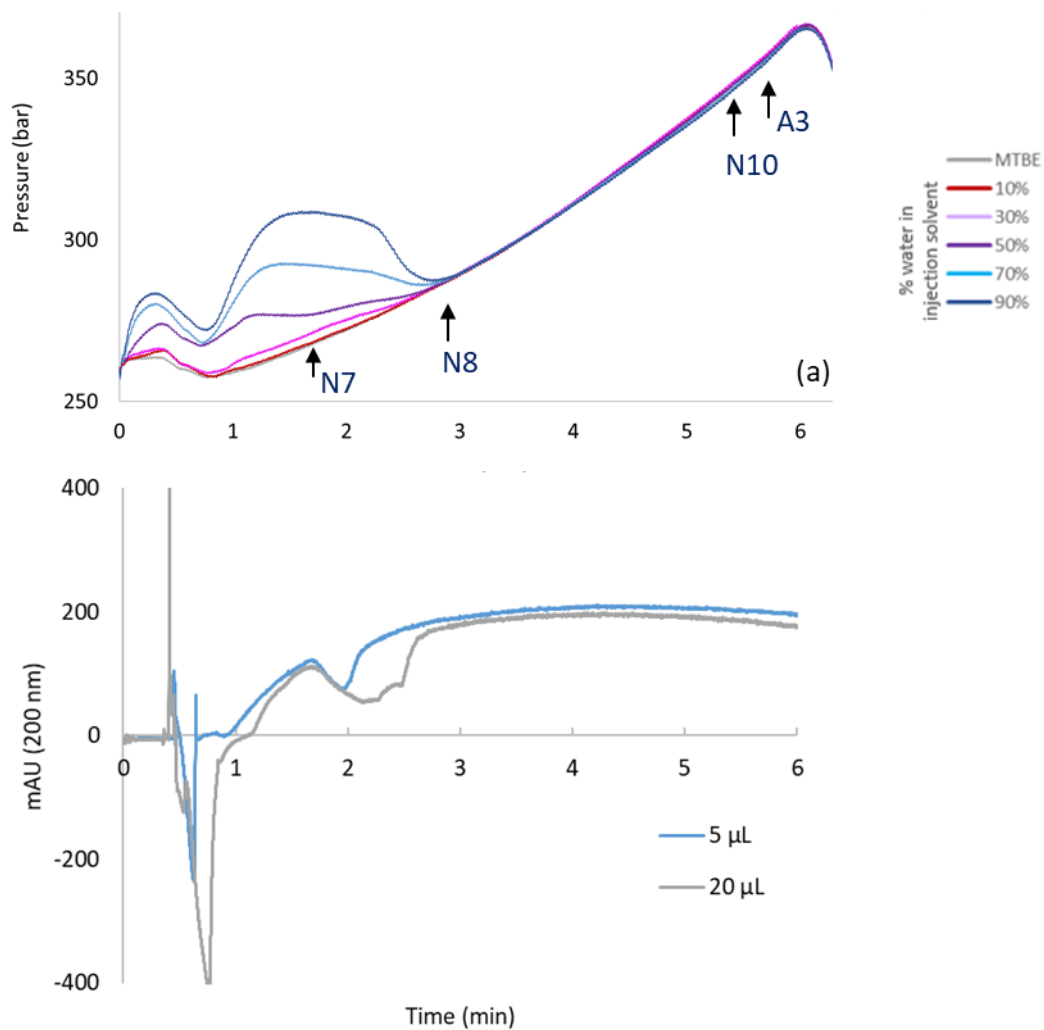
680
681
682
683
684
685
686



687
 688 Figure S4: Peak variance of the neutral test compounds, using MtBE as diluent, (a) for various organic
 689 co-solvents and (b) using MeOH with additives, i.e. 2 % water or 0.1 % formic acid additives as co-
 690 solvent. Compounds N8-N10 were not eluting during the gradient when using ACN as co-solvent.
 691
 692



693
 694
 695 Figure S5: (a) Chromatograms of two basic probes injected in ACN/water diluent with increasing
 696 content of water. UV detection 220 nm. (b) UV trace of pure water. UV detection 200 nm.
 697 Column DEA. Co-solvent MeOH + 2 % water + 20 mM ammonium hydroxide.
 698
 699
 700



701
 702
 703
 704
 705
 706
 707
 708

Figure S6: a) SFC inlet pressure when injecting 20 μL ACN/water with increasing content of water and
 b) System peaks recorded at 200 nm, when injecting 5 μL and 20 μL pure water. Column DEA. Co-
 solvent MeOH. Other conditions stated in text.

709
710
711
712

Table S1: Selected test compounds and associated composition at elution for different co-solvents.
Column DEA, gradient 5 % to 50 % co-solvent, normalized gradient slope 2 %.

Compound	Co-solvent	Composition at elution (% co-solvent)						
		MeOH	ACN/MeOH 50/50	ACN	EtOH	MeOH + 2 % H ₂ O + 0.1 % FA	MeOH + 0.1 % FA	
eugenol	N1	5.0	5.0	5.0	5.0	5.0	5.0	
2,4,6-trimethylphenol	N2	5.0	5.0	6	5.0	5.0	5.0	
1-indanol	N3	5.0	5.7	7	5.6	5.0	5.0	
apocynin	N4	6.3	7.1	11	7.4	6.5	6.3	
o-cresol	N5	7.5	8.7	14	8.8	7.3	7.5	
m-cresol	N6	8.0	9.5	16	9.4	7.8	8.1	
phenol	N7	8.5	9.9	17	9.8	8.4	8.5	
4-hydroxybenzyl alcohol	N8	17.9	36.6	21.2	20.5	18.0	18.1	
naringenin	N9	28.7	Over	31.8	32.0	27.4	28.7	
arbutin	N10	35.3	Over	42.2	38.9	34.7	35.9	
Acidic	acrylic acid	A1	21.4	29.7	Over	31.3	20.8	17.4
	trans cinnamic acid	A2	26.7	34.8	Over	37.6	25.2	19.1
	ferulic acid	A3	37.0	43.6	Over	Over	35.8	29.6
Basic	imipramine	B1	6.4	N.D.	N.D.	N.D.	N.D.	N.D.
	propranolol	B2	15.4	N.D.	N.D.	N.D.	N.D.	N.D.
	Water		13.7	13.5	N.D.*	15.6	13.9	12.3

713
714
715
716
717
718

N.D.: not determined

Over: retention over the gradient range (> 50 % co-solvent)

*The water peak could not be detected at 200 nm due to the lack of UV absorbance of ACN co-solvent.